



Journal of Agrometeorology

ISSN : 0972-1665 (print), 2583-2980 (online)
Vol. No. 24(3) : 241-248 (September 2022)

<https://journal.agrimetassociation.org/index.php/jam>



Research Paper

Assessing rice blast disease severity through hyperspectral remote sensing

NANDITA MANDAL¹, DEB K. DAS¹, RABI N. SAHOO^{1*}, SUJAN ADAK¹, A. KUMAR²,
C. VISWANATHAN³, J. MUKHERJEE¹, RAJASHEKAR⁴, RAJEEV RANJAN¹ and B. DAS¹

¹Division of Agricultural Physics ICAR-Indian Agricultural Research Institute, New Delhi-110012

²Division of Plant Pathology, ICAR-Indian Agricultural Research Institute, New Delhi-110012

³Division of plant physiology ICAR-Indian Agricultural Research Institute, New Delhi-110012

⁴ICAR-Vivekananda Parvatiya Krishi Anusandhan Sansthan, Dugalkhola, Almora, Uttarakhand-263601

*Corresponding author email: rnsahoo.iari@gmail.com

ABSTRACT

Remote sensing is being increasingly used in stress management in different agricultural practices. It is useful for real time analysis for crop stress which is not possible for visual observation alone. Rice blast caused by fungus *Pyricularia Oryzae* is a serious constrain in rice production in India. There is hardly any basic information available for spectral characteristics of rice blast disease for its real-time detection and management. Present study is to characterize spectral reflectance of blast affected rice in order to identify the sensitive spectral range. Disease severity of 10 different genotypes of rice was graded 0 to 9 based on the extent of host organ covered by symptom or lesion. Result shows that severely infected plant (score 9) have higher reflectance at visible region and lower reflectance at NIR region. Change in the reflectance for the infected plant as compare to the healthy plant was more pronounced in the VNIR, 550 to 760 nm and 1140 and 1300 nm having correlation coefficient above 0.6. The study of change in the reflectance with the change in wavelength (1st derivative) revealed that VNIR region have high correlation with the disease severity. Maximum rate of change value at red edge position (REP) is called as red edge value (REV) which has good relation with disease severity levels. Amplitude of the red edge peak decreases with the increase in severity levels. Amplitude of score 0 and 9 was 0.00929 and 0.002301, respectively for upland land condition whereas the amplitude of the score 0 and 9 was 0.010421 and 0.00193, respectively for upland land rice. This study identifies that VNIR and red edge region are sensitive for detecting rice blast, which could be utilized to aerial or satellite based monitoring blast affected rice cropping region.

Keyword: Rice, blast disease, spectral signature, red edge

Rice is the important staple food of more than half of the population of world which also holds true for India. So the failure of rice crop for any reason is threat to starvation. Rice is vulnerable to disease and pest wherever it is grown. Rice blast disease, caused by *Pyricularia oryzae*, is considered to be the most important fungal disease in rice (*Oryza sativa* L.) because of its worldwide distribution and its destruction (Couch and Kohn, 1985). The infected plant shows small brown specks of pin point size which gradually increases and developed a small roundish to slightly elongated necrotic grey spot about 1-2 mm long in diameter with distinct brown margin (IRRI, 1996). The pathogen not only destroys a single plant but completely destroys the whole field and leads to huge yield loss (Chuwa *et al.* 2015). This everlasting situation begs for proper monitoring, accurate quantification of disease severity and efficient controlling method. Traditionally the extent of diseases and pest damage in a large plant population is

assessed based on visual observation of symptomatic plants which is time consuming and labour intensive. In addition, the potentiality of raters to precisely detect plant disease may differ, as evidenced by Nutter *et al.* (1993), who turned up significant variation among raters in visually assessing dollar spot severity in creeping bentgrass (*Agrostis palustris* Huds.). Furthermore, plant responds to abiotic stress, such as drought, extreme temperatures, edaphic conditions, and high winds are difficult to quantify and thus make it difficult to assess disease severity visually with acceptable levels of accuracy and speed. However, the aforementioned plant responses to infection often affect the amount and quality of electromagnetic radiation reflected from the plant canopy (Nutter *et al.* 2002). This suggests that remote sensing techniques may provide an easily available record of disease severity and a more objective assessment than is possible with visual assessments by raters (Coops *et al.* 2003; Apan *et al.* 2004; Sankaran *et al.* 2012). Remote sensing data

Article info - DOI: <https://doi.org/10.54386/jam.v24i3.1587>

Received: 19 March 2022; Accepted: 14 July 2022; Published online: 31 August 2022

This work is licenced under a Creative Common Attribution 4.0 International licence @ Author(s), Publishing right @ Association of Agrometeorologists

especially reflectance instituted to be capable of detecting changes in the biophysical properties of plant and canopy associated with pathogens (Moran, *et al.* 1997; Moshou, *et al.* 2005; Jensen, 2007; Ranjan *et al.* 2012; Sahoo *et al.* 2015). In addition, remote sensing may provide a greater means to objectively quantify disease stress than visual assessment methods, and it can be used to repeatedly collect sample measurements non-destructively and non-invasively (Nilsson, 1995; Moran *et al.* 1997).

Characteristic changes in reflectance spectrum has been observed due to yellow rust of wheat (Bravo *et al.*, 2003), powdery mildew of wheat (Graeff *et al.* 2006), late blight of tomato (Wang *et al.* 2008), grey mold of kiwifruit (Costa *et al.* 2007), leaf roll of grapevine (Naidu *et al.* 2009) and yellow mosaic virus in soybean (Gazala *et al.* 2013). Though, commonly used broadband have been shown to detect differences between healthy and diseased plants (Sharp *et al.* 1985; Lorenzen and Jensen, 1989; Nicolas, 2004), but discrimination of healthy plants from those showing mild symptom is not very sharp. However, measurement of reflectance contiguously (hyperspectral remote sensing) as a series of narrow wavelength band provides pertinent information for discrimination of disease and other plant stresses. or remote sensing detection specific spectral reflectance associated with rice blast infection is required for large scale assessment and monitoring of blast disease in rice field especially for strategic or tactical crop management decision and yield loss prediction. However, till now no study has been conducted to characterize the reflectance spectra of rice for assessing blast disease in India. Objective of the present study was to characterize the reflectance spectra associated with blast infection

in rice for detection of the disease in large area based on remote sensing data.

MATERIAL AND METHOD

Experimental area

Field experiments were conducted in Hawalbagh farm of ICAR-Vivekananda Parvatiya Krishi Anusandhan Sansthan, Almora (29.59° N latitude, 79.64° E longitude and 1245 m above msl) at two condition of rice cultivation i.e. upland non-irrigated condition and lowland irrigated condition, with 10 genotypes of rice each for sensitive and resistance to blast disease having 3 replications laid in randomized block design (Table 1). The climate of experimental location is basically temperate type with cold winter and moderate summer. Almora has an average annual maximum temperature of around 23°C and average minimum temperature of approximately 10°C. The average annual rainfall of Almora is 1152 mm.

Measurement of spectral reflectance of rice with different gradient of blast severity

Ten rice genotypes were cultivated each for rain fed and irrigated conditions. The typical symptoms of rice blast is necrotic spot roundish elongated with a distinct brown margin which gradually covers the whole leaf. At the time of peak infection, all the rice genotypes were graded on the basis of extent of disease infection and the area covered by the necrotic lesion as per the protocol given by IRRI (1996) (Table 2).

Table 1: Disease rating score (0-9) and entries details under field conditions at Almora, Uttarakhand

Rainfed (Upland) condition		Irrigated (lowland) condition	
Entry name	Disease rating score	Entry name	Disease rating score
BL-18	9	DH-79	9
DSN-140	8	Bala	8
DSN-120	7	DH-30	7
DSN-119	6	DH-33	6
BL-21	5	DH-34	5
BL-6	4	DH-32	4
BL-10	3	DH-44	3
BL-12	2	DH-49	2
VL 32473	1	DH-47	1
VL 32475	0	DH-94	0

Table 2: Description of disease score of blast disease of rice crop as per the protocol given by IRRI (1996)

Disease rating	Description
Score 0	No lesion
Score 1	Small brown specks of pin point size
Score 2	Small roundish to slightly elongated, necrotic gray spots, about 1-2 mm in diameter, with a distinct moderately resistant brown margin. Lesions are mostly spotted on the lower leaves
Score 3	Lesion type is same as in 2, but significant number of lesions on the upper leaves
Score 4	Typical susceptible blast lesions, 3 mm or longer infecting $\leq 4\%$ of leaf area
Score 5	Typical susceptible blast lesions of 3 mm or longer infecting 4-10% of the leaf area
Score 6	Lesion type is same as in score 5 but infecting about 11-25% of the leaf area
Score 7	Lesion type is same as in score 5 infecting about 26-50% of the leaf area
Score 8	Typical susceptible blast lesions of 3 mm or longer infecting about 51-75% of the leaf area many leaves are dead
Score 9	Typical susceptible blast lesions of 3 mm or longer infecting $\geq 75\%$ leaf area affected

Canopy reflectance of rice at Almora field was measured for 10 (0-9 scale) disease severity levels with help of hand held ASD FieldSpec spectroradiometer (Analytical Spectral Devices Inc., Boulder, CO, USA). The measurement was taken on a clear sunny day between 11.00am - 01.00 pm with spectroradiometer having a 25° field of view and positioned at 0.5 m from the top of the canopy at nadir position in the spectral arrange of 350-2500 nm. Prior to spectral reflection measurement the instrument was optimized with white reference panel called spectralon (Labsphere, Inc., Sutton, NH, USA) and reference reflectances were measured followed by canopy reflectance measurements. Each spectral measurement is the average of the 30 spectral scan of the sample. Instrument optimization was repeated with the spectralon in between the spectral observations when there was a change in sun light conditions.

Pre-processing of spectral reflectance data

The aim of pre-processing is to reduce the effects of random noise and improve signal-to noise ratio. The most frequently used filter in spectral data analysis is Savitzky-Golay filter that uses a moving polynomial fit of any order and the size of the filter is calculated as $(2n+1)$ points, where n is the half-width of the smoothing window. The points between the $2n$'s are interpolated by the polynomial fit (Savitzky and Golay, 1964).

Developing relationship between spectral reflectance and disease severity

The correlation between spectral reflectance and disease severity was analyzed to identify the different spectral regions sensitive to rice blast disease. In this study the correlation value 0.6 was considered as threshold to identify the sensitive spectral regions.

Spectral derivative and red edge analysis

First derivative of mean reflectance was calculated and appropriate order of polynomial fitting was performed through least squares method (Savitzky and Golay, 1964). Red edge shifts and shapes of the red peak in the first derivative curve were studied under various levels of disease severity. Wavelength (k_{re}) and amplitude (dr_{re}) of the red peak for each infection level were estimated through linear interpolation technique by fitting a second order polynomial equation to the red infrared slope (Guyot *et al.* 1988). Characterization of spectra under different severity levels was done in relation to the following red edge parameters; λ_{re} the wavelength of this red edge peak, dr_{re} the amplitude of the red edge peak in the first derivative reflectance curve and $\Sigma(dr\ 670-780)$ sum of the first derivative reflectance amplitudes between 670 and 780 nm.

RESULT AND DISCUSSION

Scoring of blast disease infection

The disease severity levels were estimated by evaluating percentage of host tissue covered by the necrotic lessons of the disease and number and size of the lesson. The extent of rice blast severity was graded from 0-9 as per the guideline of IRRI. The severity level 0 depicts that the plant is healthy having no symptoms

at all and the disease severity level 9 depicts that the plant is most severely affected by pathogen. The disease severity levels; in-between show various levels of infestation and severity level gradually increases from 0 to the level 9. Rice genotypes, BL 18 and DH 79 grown under rain fed and irrigated conditions respectively were assigned as level 9. Genotypes, VL 32475 and DH 94 grown under rain fed and irrigated conditions respectively were assigned as severity level 0. The details of other variety and their corresponding severity levels are shown in Table 1.

Response of leaf reflectance to variation in disease severity level

In this study a differential spectral response was witnessed with varying level of disease infestation. Fig. 1 shows the dynamic changes in leaf reflectance under different disease infestation levels. As the disease severity level progressed, the reflectance in visible region increases, basically at the red region the reflectance is more in the severely affected plant than the healthy plant. At this particular spectral region the spectral reflectance was mainly influenced by leaf pigment content. For blast infected plants, plant chlorophyll was almost damaged by the pathogen. Similar finding was also investigated by Kobayashi *et al.* (2003) for panicle blast disease detection. In the NIR region the reflectance of healthy plant is higher than infected and with the increase in disease severity level reflectance at NIR region gradually decreased. Due to the severe infection by the pathogen, the plant eventually starts producing the reactive oxygen species such as hydrogen peroxide and deposition of cellulose at the site of infection (Thordal-Christensen *et al.* 1997; Nishimura *et al.* 2003) which are the main causes of producing necrotic lesions leading to cell damage and finally death of the plant. Das *et al.* (2013) also reported the decrease in reflectance at NIR region for yellow mosaic virus infected soybean crop. In the SWIR region there was higher reflectance for the severely affected plant as compare to the disease infected plant. This may be attributed to the lower leaf water content for the blast infected plants.

The difference of reflectance of rice plant at different severity levels (score 1 to 9) from that of healthy plant was computed and plotted over spectral range 350 to 2500nm (Fig. 2). The spectral ranges where difference is very conspicuous are red band at around 690nm and NIR ranging from 800 to 1100 nm. More the severity more is the in positive difference in red band and more in negative difference in the NIR range. In shortwave infrared region also positive difference in reflectance was found. Absorption in visible range 400-700nm is mainly characterized by electron transitions in chlorophyll and other plant pigments. In NIR and SWIR spectral ranges, spectral reflectance gets major affected by bending and stretching of the O-H bond in water and other molecules yielding unique absorption centred at wavelengths of 970nm, 1145nm, 1400nm and 1940nm (Curran, 1989) Spectral reflectance in the near infrared region (700-1100nm) is dependent mostly on the internal leaf structure. In NIR spectral range, there are multiple reflections in the internal mesophyll structure caused by differences in the refractive index of cell wall and the internal air cavity namely vacuole so normally plant experience higher reflectance. At the short wave infrared region (1100-2500nm) reflectance is influenced by composition of leaf chemical and water (Jacquemoud and Ustin, 2001).

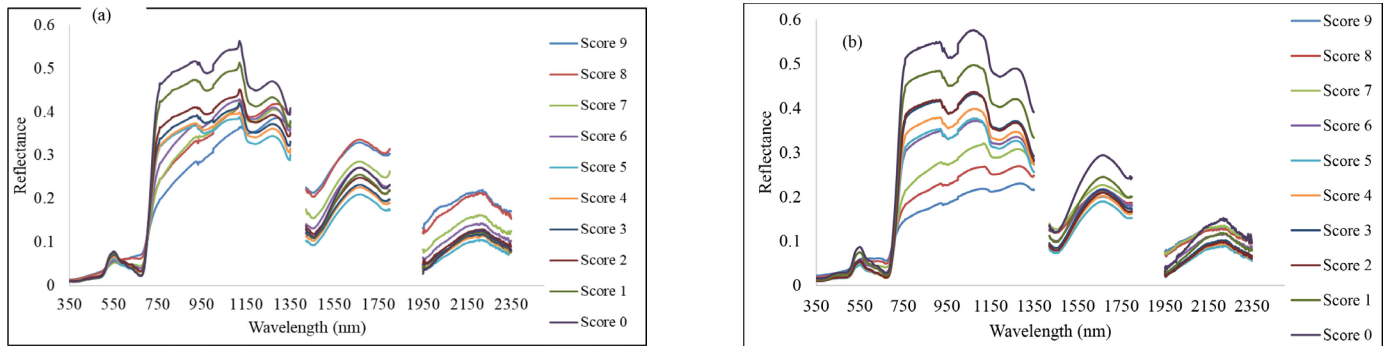


Fig. 1: Spectral reflectance of rice canopy under different disease severity levels at Almora under (a) Rainfed (upland) and (b) Irrigated (lowland) conditions

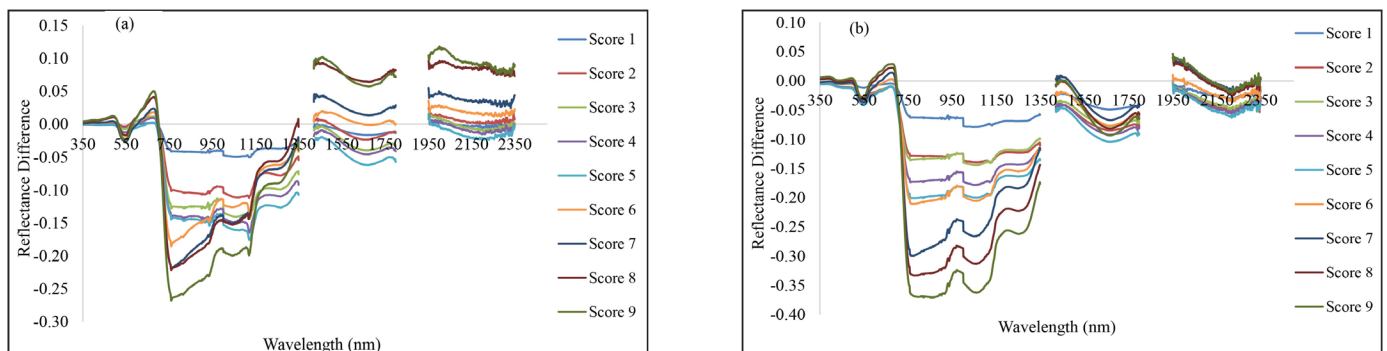


Fig. 2: Spectral reflectance difference of rice plant with different severity levels with reference to healthy (a) Rainfed (upland), (b) Irrigated (lowland)

Relationship between disease severity and spectral reflectance

Spectral reflectance at each wavelength was variably correlated with the disease severity score values *i.e.* 0 to 9 over the whole spectral range (350 to 2500 nm) (Fig. 3). Considering correlation above 0.6 as threshold value, identifies spectral ranges having relation with disease scores are at 690nm, 700 to 1000nm and at 1475nm and 1950 to 2100 nm in case genotypes grown under upland condition. Similar relation was also found in low land condition of rice grown except at SWIR-1 where relation was poor. Evaluating the spectral reflectance of rice blast at their different severity levels revealed significant difference in the reflected values in visible, NIR and SWIR spectral ranges though reflectance pattern remains same.

Rice blast is caused by hemibiotrophic fungi. The pathogen produces a specialized infectious structure called appressorium, which adheres tightly the plant surface using mucilage (Howard *et al.* 1991). The fungus generates enormous turgor pressure inside the leaf cell and thin penetration peg pierces the rice leaf surface using this pressure to enter into the host by damaging the epidermal and mesophyll cell, that hyphae then starts growing intracellular and inter cellular by slowly damaging the internal leaf structure. Due to the severe infection by the pathogen, the plant eventually starts producing the reactive oxygen species such as hydrogen peroxide and deposition of callose at the site of infection (Thordal-Christensen *et al.* 1997; Nishimura *et al.* 2003) which are the main causes of producing necrotic lesions leading to cell damage and

finally death of the plant. Callose is a plant polysaccharide produced to act as a temporary cell wall in response to disease stress. This is reason of significant changes in spectral reflectance values in NIR ranges. Pathogen severely affects the mesophyll cell and almost kills the plant. Therefore, at the disease severity level 9, there is no difference between spectra of soil and plant as the plant is almost dead. These observations are aligned with results reported by Yang *et al.* (2012) for blast disease in rice.

Response and relationship of 1st derivative of canopy reflectance to variation in disease severity

By plotting the change in reflectance with respect to the change in wavelength (1st derivative) the sensitive spectral ranges of disease severity assessment was calculated (Fig. 4), and then correlated with disease severity scores (Fig. 5). It was found that correlation was higher ($r > 0.6$) in visible and NIR ranges whereas a lower correlation was found in case of SWIR I and SWIR II region. A higher and positive correlation was found in the region of 490-550 and 680-760 nm whereas 550-680 nm region was negatively correlated. The correlation was also higher at few spectral values in the ranges of 1100-1200 and 1250-1340 nm. Mathematical transformation of the reflectance to 1st derivative led to identify some of the sensitive spectral ranges to rice blast disease severity levels. Evaluating the red edge region of the spectral reflectance (680-760nm) from 1st derivative reflectance values, high correlation of

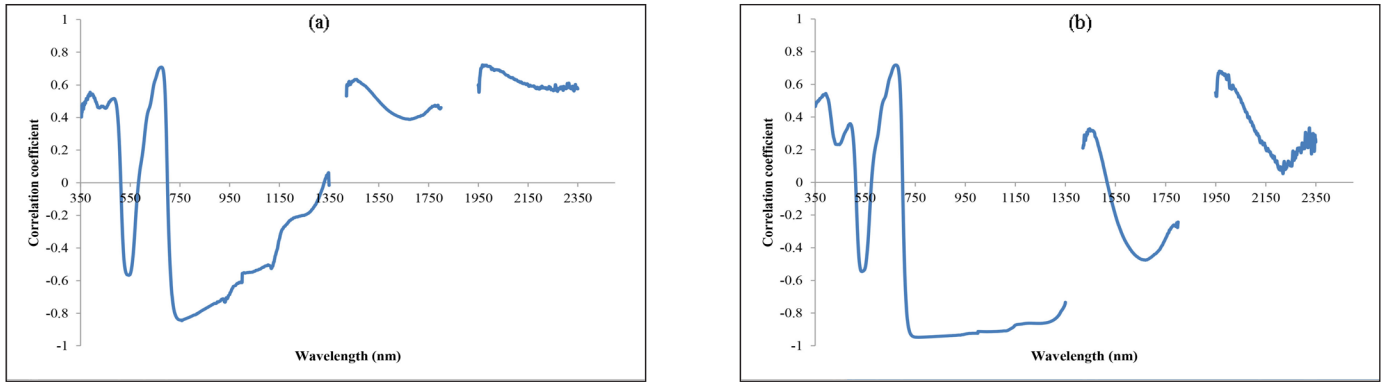


Fig. 3: Correlation between canopy reflectance and disease severity (a) Rainfed (upland), (b) Irrigated (lowland)

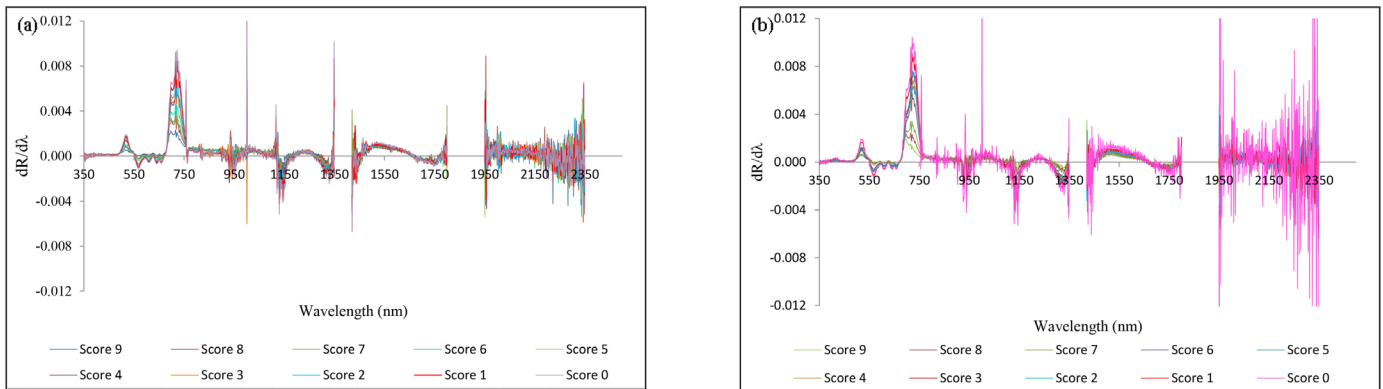


Fig. 4: 1st derivative of canopy reflectance spectra of blast infected rice at different severity level (a) Rainfed (upland) and (b) Irrigated (lowland)

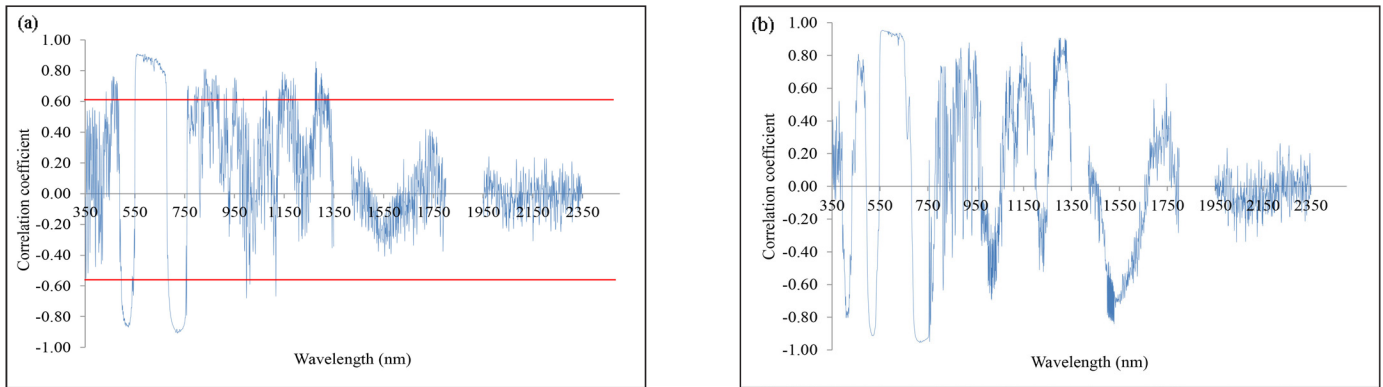


Fig. 5: Sensitive spectral ranges for disease severity through correlation analysis of 1st derivative of spectral reflectance with disease score values in (a) Rainfed (upland) and (b) Irrigated (lowland)

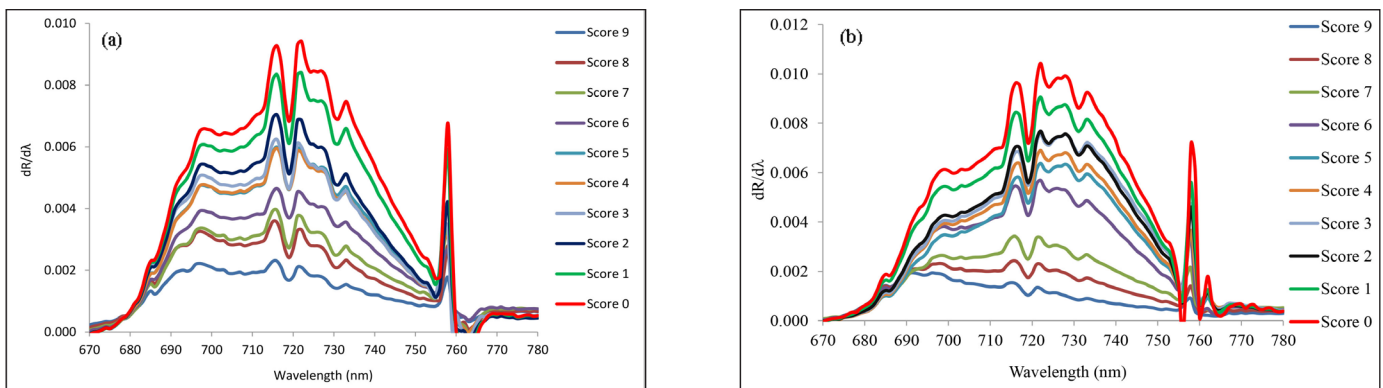
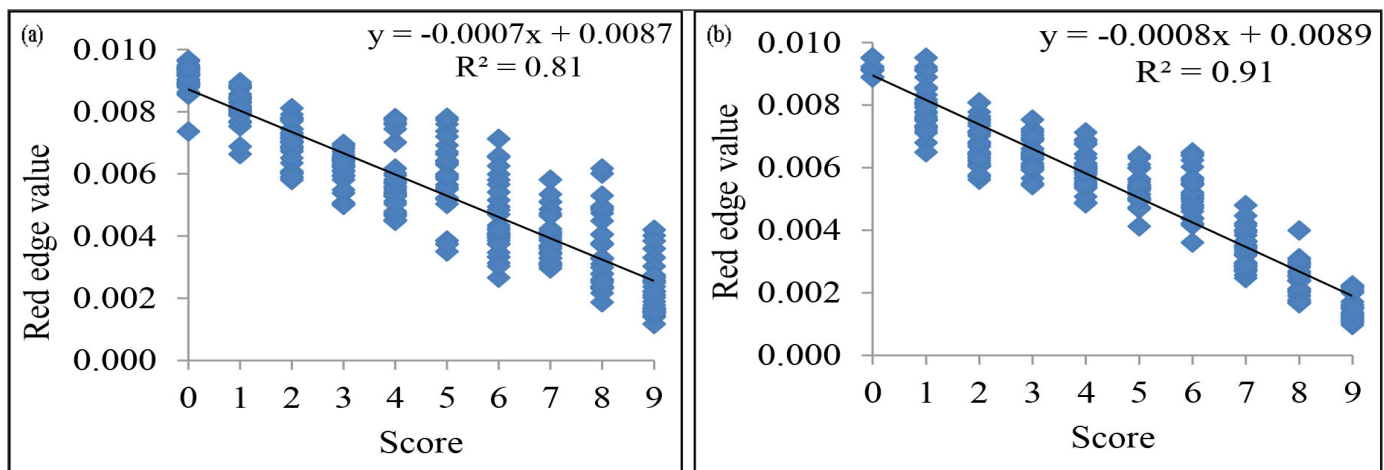


Fig. 6: Red edge curve of blast infected rice canopy in (a) Rainfed (upland) and (b) Irrigated (lowland)

Table 3: Characteristics of red edge curve under different disease severity levels

Disease score	Rainfed (upland) condition		Irrigated (lowland) condition	
	Amplitude of red edge peak (REV)	Sum of the first derivative reflectance amplitudes between 670 and 780 nm	Amplitude of red edge peak (REV)	Sum of the first derivative reflectance amplitudes between 670 and 780 nm
9	0.002301	0.14037	0.001935	0.09902
8	0.003579	0.19416	0.002420	0.14089
7	0.003948	0.21308	0.003414	0.18379
6	0.004648	0.25566	0.005692	0.28623
5	0.005993	0.30546	0.006378	0.31054
4	0.005954	0.30184	0.006897	0.33602
3	0.006242	0.31344	0.007551	0.37090
2	0.007041	0.33868	0.007677	0.37004
1	0.008400	0.40711	0.009063	0.43803
0	0.009429	0.45032	0.010421	0.49294

**Fig. 7:** Relationship between disease severity level (score) and red edge value (REV) (a) Rainfed (upland), (b) Irrigated (lowland)

red edge value (REV) with disease scores was found. Correlations of 1st derivative of spectral reflectance with disease scores confirmed again sensitivity of red edge region with disease severity levels. The pathogen of rice blast damages the cell structure and dries of the plant producing necrotic spots. The damage in chlorophyll content of plant led to effect on red edge value. Cell structure damage and loss of cell water led to high correlation of disease score values in spectral range in NIR and SWIR ranges 1100-1200nm and 1250 to 1340nm. The mixed effect of loss of plant chlorophyll and damage of cellular structure yielded this VNIR as most the sensitive region for disease detection.

Effect of disease severity on spectral reflectance in red edge region

Red edge region is the spectral range from 680 to 760 nm (Fig. 6). The rate of change of reflectance with wavelength in the red edge region is very sensitive for detection of stress of a crop. The point of inflection where rate of change of reflectance changes from positive to negative is called red edge position (REP). REP shifts to lower spectral value called blue shift when there is stress and it shifts to higher value called red shift when the plant recovers from stress basically healthy. Though there was no evidence of blue shift

with the increase in blast severity levels in this study. Amplitude of the red edge peak decreases with the increase in severity levels. Amplitude of score 0 and 9 was 0.00929 and 0.002301, respectively for upland land condition whereas the amplitude of the score 0 and 9 was 0.010421 and 0.00193, respectively for upland land rice (Table 3). Fahrenttrapp *et al.* (2019) and Adak *et al.* (2021) reported similar findings for gray mold leaf infections and nitrogen stress in wheat, respectively. Max rate of change value at REP is called red edge value (REV) which has good relation with stress levels. REV is maxima of 1st derivative reflectance. The regression analysis between REV and disease severity score showed a high R² value of 0.81 and 0.91 for upland and irrigated condition, respectively (Fig 7). Table 3 shows that the sum of first derivative reflectance between 670-780 nm gradually decreases towards the highest disease severity level. This is consistent with findings by Mahlein *et al.* (2010) who found similar red edge reflection patterns studying sugar beet leaves infected with fungal diseases such as *C. beticola* and *U. betae*.

CONCLUSIONS

The study revealed potential of hyperspectral remote

sensing not only for characterizing rice crop infected with blast disease but also finding out sensitive bands to assess its severity level. Difference in spectral reflectance was clearly visible for different disease severity levels and was more pronounced in VNIR range. Spectral transformation to 1st derivative (red edge) and 2nd derivative led to find most sensitive spectral ranges 550 to 760nm and 1140 and 1300 nm for disease scores. Predictive model blast disease with red edge value (REV) with R² value 0.81 and 0.91 revealed above 0.6 has great opportunity to upscale in field scale using some the recently develop multispectral camera with red edge band on airborne platform like unmanned aerial vehicles.

ACKNOWLEDGEMENT

Authors acknowledges Post Graduate School, ICAR-Indian Agricultural Research Institute, New Delhi for research fellowship and Divisions of Agricultural Physics, Plant Pathology and Plant Physiology, ICAR-IARI, New Delhi, and ICAR-VPKAS, Almora for extending research facilities.

Conflict of Interest Statement: The author (s) declares (s) that there is no conflict of interest.

Disclaimer: The contents, opinions and views expressed in the research article published in Journal of Agrometeorology are the views of the authors and do not necessarily reflect the views of the organizations they belong to.

Publisher's Note: The periodical remains neutral with regard to jurisdictional claims in published maps and institutional affiliations.

REFERENCES

- Adak, S., Bandyopadhyay, K.K., Sahoo, R.N., Mridha, N., Shrivastava, M. and Purakayastha, T.J. (2021). Prediction of wheat yield using spectral reflectance indices under different tillage, residue and nitrogen management practices. *Curr. Sci.*, 121(3): 402-413.
- Apan, A., Held, A., Phinn, S. and Marley, J. (2004). Detecting sugarcane 'orange rust' disease using EO-1 Hyperion hyperspectral imagery. *Int J Remote Sens.*, 25: 489-98.
- Bravo, C., Moshou, D., West, J., McCartney, A. and Ramon, H. (2003). Early disease detection in wheat fields using spectral reflectance. *Biosyst. Eng.*, 84 (2):137-145.
- Chuwa, C.J., Mabagala, R.B. and Reuben, M.S.O.W. (2015). Assessment of grain yield losses caused by rice blast disease in major rice growing areas in Tanzania. *Int. J. Sci. Res.*, 4(10): 2211-2218.
- Coops, N., Stanford, M., Old, K., Dudzinski, M., Culvenor, D. and Stone, C. (2003). Assessment of Dothistroma needle blight of *Pinus radiata* using airborne hyperspectral imagery. *Phytopathol.*, 93(12): 1524-1532.
- Costa, G., Noferini, M., Fiori, G. and Spinelli, F. (2007). Innovative application of non-destructive techniques for fruit quality and disease diagnosis. *Acta Hort.*, 753(1): 275.
- Couch, B.C. and Kohn, L.M.A. (1985). Multilocus gene genealogy concordant with host preference indicates segregation of a new species, *Magnaporthe oryzae*, from *M. grisea*. *Mycologia*, 94(4): 683-93.
- Curran, P.J. (1989). Remote sensing of foliar chemistry. *Remote Sens. Environ.*, 30(3): 271-278.
- Das, D.K., Pradhan, S., Sehgal, V.K., Sahoo, R.N., Gupta, V.K., Singh, R. (2013). Spectral reflectance characteristics of healthy and yellow mosaic virus infected soybean (*Glycine max* L.) leaves in a semiarid environment. *J. Agrometeorol.*, 15(1): 36-38. <https://doi.org/10.54386/jam.v15i1.1435>
- Fahrentrapp, J., Ria, F., Geilhausen, M. and Panassiti, B. (2019). Detection of gray mold leaf infections prior to visual symptom appearance using a five-band multispectral sensor. *Front. Plant Sci.*, 10:628-635
- Gazala, I.F., Sahoo, R.N., Pandey, R., Mandal, B., Gupta, V.K., Singh, R. and Sinha, P. (2013). Spectral reflectance pattern in soybean for assessing yellow mosaic disease. *Indian J Virol.*, 24(2): 242-249.
- Graeff, S., Link, J. and Claupein, W. (2006). Identification of powdery mildew (*Erysiphe graminis* sp. tritici) and take-all disease (*Gaeumannomyces graminis* sp. tritici) in wheat (*Triticum aestivum* L.) by means of leaf reflectance measurements. *Open Life Sci.*, 1(2): 275-288.
- Guyot, G., Baret, F. and Major, D.J. (1988). High spectral resolution: determination of spectral shifts between the red and the near infrared. *Int Arch. Photogramm Rem. Sens.*, 11: 750-60.
- Howard, R.J., Bourett, T.M. and Ferrari, M. A. (1991). Infection by *Magnaporthe*: an in vitro analysis. In *Electron microscopy of plant pathogens*, Springer, Berlin, Heidelberg, pp. 261-264.
- IRRI (1996). <http://www.knowledgebank.irri.org/images/docs/rice-standard-evaluation-system.pdf>
- Jacquemoud, S. and Ustin, S.L., 2001, January. Leaf optical properties: A state of the art. In 8th International Symposium of Physical Measurements & Signatures in Remote Sensing (pp. 223-332). CNES Aussois France.
- Jensen, J.R. (2007). Remote sensing of the environment: an earth resources perspective. 2nd ed. New Jersey: Pearson Education, Inc. 12-56.
- Kobayashi, T., Kanda, E., Naito, S., Nakajima, T., Arakawa, I., Nemoto, K., Honma, M., Toujyou, H., Ishiguro, K., Kitada, K. and Torigoe, Y. (2003). Ratio of rice reflectance for estimating leaf blast severity with a multispectral radiometer. *J. Gen. Plant Pathol.*, 69(1): 17-22
- Lorenzen, B. and Jensen, A. (1989). Change in leaf spectral

- properties induces in barley by cereal powdery mildew. *Rem Sens Environ.*, 27: 201–9.
- Mahlein, A.K., Steiner, U., Dehne, H.W., and Oerke, E.C. (2010). Spectral signatures of sugar beet leaves for the detection and differentiation of diseases. *Precis. Agric.*, 11: 413–431
- Moran, S., Inoues, Y and Barnes, E.M. (1997). Opportunities and limitation for image-based remote sensing in precision farming. *Rem Sens Environ.*, 61: 319–46.
- Moshou, D., Bravo, C., Oberti, R., West, J., Bodria, L., McCartney, A. and Ramon, H. (2005). Plant disease detection based on data fusion of hyper-spectral and multi-spectral fluorescence imaging using Kohonen maps. *Real-Time Imaging*, 11(2): 75-83.
- Naidu, R.A., Perry, E.M., Pierce, F.J. and Mekuria, T. (2009). The potential of spectral reflectance technique for the detection of Grapevine leafroll-associated virus-3 in two red-berried wine grape cultivars. *Comput Electron Agric.*, 66(1): 38-45.
- Nicolas, H. (2004). Using remote sensing to determine of the date of a fungicide application on winter wheat. *Crop Prot.*, 23(9): 853-863.
- Nilsson, H. (1995). Remote sensing and image analysis in plant pathology. *Annual Review Phytopathol.*, 33(1): 489-528.
- Nishimura, M.T., Stein, M., Hou, B.H., Vogel, J.P., Edwards, H. and Somerville, S.C. (2003). Loss of a callose synthase results in salicylic acid-dependent disease resistance. *Science*, 301(5635): 969-972.
- Nutter Jr, F.W., Gleason, M.L., Jenco, J.H. and Christians, N.C. (1993). Assessing the accuracy, intra-rater repeatability, and inter-rater reliability of disease assessment systems. *Phytopathol.*, 83(8): 806-812.
- Nutter Jr, F.W., Guan, J., Gotlieb, A.R., Rhodes, L.H., Grau, C.R. and Sulc, R.M. (2002). Quantifying alfalfa yield losses caused by foliar diseases in Iowa, Ohio, Wisconsin, and Vermont. *Plant Dis.*, 86(3): 269-277.
- Ranjan, R., Chopra, U.K., Sahoo, R.N., Singh, A.K. and Pradhan, S. (2012). Assessment of plant nitrogen stress in wheat (*Triticum aestivum* L.) through hyperspectral indices. *Int. J. Remote Sens.*, 33(20): 6342-6360.
- Sahoo, R.N., Ray, S.S. and Manjunath, K.R. (2015). Hyperspectral remote sensing of agriculture. *Curr. Sci.*, pp.848-859.
- Sankaran, S., Ehsani, R., Inch, S.A. and Ploetz, R.C. (2012). Evaluation of visible-near infrared reflectance spectra of avocado leaves as a non-destructive sensing tool for detection of laurel wilt. *Plant Dis.*, 96(11): 1683-1689.
- Savitzky, A. and Golay, M.J. (1964). Smoothing and differentiation of data by simplified least squares procedures. *Anal. Chem.*, 36(8): 1627-1639.
- Sharp, E.L., Perry, C.R., Scharen, A.L., Boatwright, G.O., Sands, D.C., Lautenschlager, L.F., Yahyaoui, C.M. and Ravet, F.W. (1985). Monitoring cereal rust development with a spectral radiometer. *Phytopathol.*, 75(8): 936-939.
- Thordal-Christensen, H., Zhang, Z., Wei, Y. and Collinge, D.B. (1997). Subcellular localization of H₂O₂ in plants. H₂O₂ accumulation in papillae and hypersensitive response during the barley—powdery mildew interaction. *Plant J.*, 11(6): 1187-1194.
- Wang, X., Zhang, M., Zhu, J. and Geng, S. (2008). Spectral prediction of *Phytophthora infestans* infection on tomatoes using artificial neural network (ANN). *Int. J. Remote Sens.*, 29(6): 1693-1706.
- Yang, Y., Chai, R. and He, Y. (2012). Early detection of rice blast (*Pyricularia*) at seedling stage in Nipponbare rice variety using near-infrared hyper-spectral image. *Afr. J. Biotechnol.*, 11(26): 6809-6817.